Int. J. Electrochem. Sci., 15 **(2020)** 10802 – 10815, doi: 10.20964/2020.11.17

International Journal of
ELECTROCHEMICAL
SCIENCE
www.electrochemsci.org

Inhibition of Under-Deposit Corrosion of Carbon Steel by Bupropion Drug in CO_2 Saturated Brine Solutions

Ali Sorkh Kaman Zadeh, Mehdi Shahidi-Zandi[*]*, Maryam Kazemipour*

Department of Chemistry, Kerman Branch, Islamic Azad University, Kerman, Iran.
[*]E-mail: meshahidizandi@gmail.com; shahidi@iauk.ac.ir

Received: 15 June 2020 / *Accepted:* 28 July 2020 / *Published:* 30 September 2020

Inhibition effects of bupropion drug on the under-deposit corrosion of carbon steel in 3.5% NaCl solution saturated with CO_2 have been investigated by the techniques of potentiodynamic polarization and electrochemical impedance spectroscopy (EIS). The sand-covered electrode was prepared by covering the carbon steel electrode with a layer of the silica sand. The increase of the drug concentration up to 600 ppm led to increasing the inhibition efficiency of carbon steel against under-deposit corrosion in the brine solution. Further increasing of the bupropion concentration caused the lowering of the inhibition efficiency. The Langmuir isotherm can describe the adsorption behavior of bupropion on the surface of carbon steel. Measurements of potentiodynamic polarization indicated that bupropion is an anodic inhibitor. The effects of temperature on the under-deposit corrosion behavior of carbon steel were studied both in the absence and presence of 600 ppm bupropion drug. The enthalpy of the drug adsorption was obtained from the temperature dependence of the corrosion inhibition process. A reasonable agreement was observed between the IE values resulted from the potentiodynamic polarization and the EIS techniques.

Keywords: Bupropion drug; Under-deposit corrosion (UDC); Corrosion of oil pipelines; Electrochemical impedance spectroscopy; Potentiodynamic polarization.

1. INTRODUCTION

The corrosion of steel pipelines of oil and gas increases by settling of deposits such as sand in them. It is very important to consider this type of corrosion, namely as the under-deposit corrosion (UDC), because of the pipeline leaking effect of it [1, 2].

Because of the presence of carbon dioxide gas in the oil wells, it is worth considering the CO_2 corrosion as a major challenge in the natural gas and oil industries [3-5]. The literature survey reveals a lot of papers on the CO_2 corrosion of steel alloys [3-15]. The CO_2 corrosion of the steel alloys has shown more severe corrosion in comparison with the same pH acidic solutions [14].

The main cathodic reactions in the CO_2 corrosion can be the reduction of H^+, H_2CO_3, HCO_3^- and H_2O [16]. Despite some debate in the literature, the hydrogen reduction reaction (HER) has been agreed as the predominant cathodic reaction at the pH range of 3 to 5.5 [17]. The Fe dissolution as the main anodic reaction involves an adsorbed intermediate as the rate-determining step [18].

The corrosion inhibitors, as the most common protecting materials for CO_2 corrosion of carbon steel [19], are substances whose small concentrations prevent the corrosion of the alloys by the corrosive media. The molecular structure of the most popular corrosion inhibitors contains S, N, O, P atoms and aromatic rings [20]. The experiments of the sand adsorption have shown that the tendency of the corrosion inhibitors to adsorb on a sand substrate depends on their chemical nature [21]. Sulfur-containing inhibitors indicate a lower tendency to adsorb on the sand substrate than to adsorb on the steel surface.

In this paper, bupropion drug was investigated as an inhibitor against under-deposit corrosion of carbon steel in 3.5% NaCl solution saturated with CO_2 by the techniques of potentiodynamic polarization and impedance spectroscopy.

2. MATERIALS AND METHODS

2.1 Materials

Bupropion drug and silica sand (SiO_2) were supplied from Sigma Aldrich. Sodium chloride was prepared from Merck. The molecular structure of the bupropion is shown in Figure 1. The working electrode used here is made of carbon steel with a surface area of 1.0 cm^2.

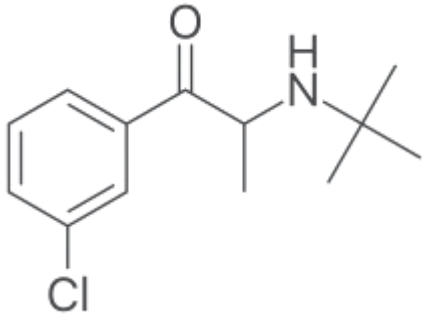

Figure 1. Structure of bupropion.

2.2 Methods

10 g of the acid-washed silica sand was used in all experiments. The working electrode (WE) was located at the bottom of the test cell containing the brine solution and suspended silica sand to provide the sand-covered electrode simulating the sand settling in the oil pipelines. The corrosive solution was CO_2 saturated 3.5% NaCl solution. The solutions under stagnant conditions were employed for the measurements.

The potentiodynamic polarization and impedance measurements were used to investigate the corrosion rate of carbon steel in the CO_2 saturated 3.5% sodium chloride solutions both in the absence and presence of different amounts of bupropion drug. Before performing the tests, the surface of the sample was rubbed with wet sandpapers through different grades then washed with distilled water and at last dried in air. The sample, as the working electrode, was sealed by epoxy resin at one side after connecting a copper wire to it.

An Autolab 302N potentiostat equipped with Nova 1.9 software was used for potentiodynamic polarization and EIS tests. The counter electrode (CE) was prepared from a platinum rod and the reference electrode was a saturated (KCl) Ag/AgCl electrode. The electrochemical test order was EIS and afterward the polarization technique. Before performing the tests, the specimens were soaked in the solution for about 30 minutes to stabilize the open circuit potential (OCP).

For the EIS tests, a sinusoidal potential signal of 10 mV (vs OCP) was used in the frequency range of 100 kHz-10 mHz. Potentiodynamic polarization curves were obtained by changing the potential from -300 to + 300 mV vs. OCP with the scan rate of 1 mV/s. Nova 1.9 software was employed for both analyzing the Nyquist plots of EIS data and determining the polarization parameters arising from Tafel curves.

3. RESULTS AND DISCUSSION

3.1 Potentiodynamic polarization measurements

Figure 2 shows the Tafel plots of carbon steel exposed to CO_2 saturated NaCl solutions containing different amounts of bupropion. Since the cathodic branch displays a Tafel behavior it is possible to make an accurate evaluation of both the cathodic Tafel slope (β_c) and the corrosion currents (j_{corr}) by the Tafel extrapolation method [22]. On the other hand, the expected log/linear Tafel behavior is not displayed by the anodic polarization curve over the applied potential range. The deposition of the corrosion products or impurities in the carbon steel (e.g., Fe_3C) and the formation of a non-passive film may be the reason for the curvature of the anodic branch [23]. Therefore, due to the curvature of the anodic branch, it is not suitable to evaluate the anodic Tafel slope by Tafel extrapolation of the anodic branch of the polarization plot.

In the Tafel extrapolation method, it preferred to use both the anodic and cathodic Tafel regions rather than only one Tafel region [24]. However, it is also possible to use the Tafel extrapolation of either the cathodic or anodic branch alone to determine the corrosion rate. In this condition, the cathodic branch is preferred due to the long defined Tafel region of it (as in our case here).

The anodic current density can be calculated from the experimental data. For this purpose, after extending the Tafel line of the cathodic branch to zero overvoltage, the following equation was employed to calculate the anodic current density [24]:

$$i_a(\text{net exp}) = i_a - |i_c| \quad (1)$$

where the subscripts a and c refer the anodic and cathodic terms, respectively. Thus, the anodic current density, i_a , is obtained from the sum of the net experimental anodic current density, $i_a(\text{net exp})$, and the extrapolated cathodic current density, $|i_c|$.

Table 1 lists the current density (i_{corr}), the Tafel slopes (β_a, β_c) and corrosion potential (E_{corr}).

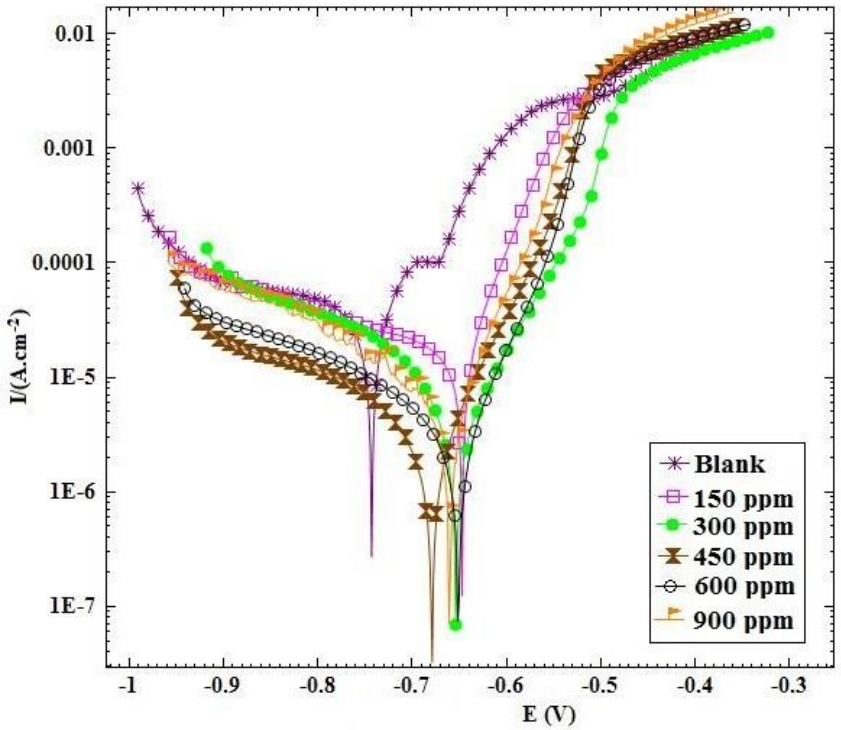

Figure 2. Polarization curves of carbon steel in CO_2 saturated brine solution with different concentrations of bupropion at 25°C.

Table 1. Polarization parameters and the corresponding inhibition efficiencies for carbon steel in 3.5% NaCl solution saturated with CO_2 in the absence and presence of different concentrations of bupropion drug at 25°C.

C /ppm	i_{corr}/μA.cm^{-2}	-E_{corr}/mV	β_a/mV.decade^{-1}	β_c/mV.decade^{-1}	IE_P(%)
0	30.8	744	102	956	-
150	8.5	648	54	324	72.4
300	4.8	654	70	148	84.4
450	3.3	680	63	237	89.3
600	2.8	652	57	183	90.9
900	3.8	661	54	148	87.7

As it is clear from Figure 2, the anodic current density was found to decrease significantly after the addition of inhibitor, while the cathodic current density changed slightly after the inhibitor addition. Besides, it can be seen that the potential of corrosion changed to more positive values in the presence of inhibitor. Generally, the corrosion inhibitor will be considered as the cathodic or anodic type if the change in the absolute value of E_{corr} is more than 85 mV with respect to E_{corr} of the blank solution, and if the shift is less than 85 mV, the inhibitor can be classified as a mixed type [25-27]. In the present work, the maximum change in equilibrium corrosion potential was about +95 mV,

suggesting that the bupropion can be known as an anodic inhibitor. This result is consistent with the above result that the anodic current density of the steel electrode in CO_2 saturated brine solution is significantly reduced by the addition of the inhibitor.

Table 1 shows the inhibition efficiency (IE) values expressed by the following equation [28]:

$$IE_P(\%) = \frac{i_{corr} - i'_{corr}}{i_{corr}} \times 100 \quad (1)$$

where i_{corr} and i'_{corr} are current densities of corrosion in the blank and the inhibited solutions, respectively. The IE_P values increased with increasing the bupropion concentration and reached the maximum value for 600 ppm of bupropion. Further increasing of the bupropion concentration up to 900 ppm caused the lowering of the IE_P values. These values indicate that the drug acts as an effective inhibitor for preventing the under-deposit corrosion of carbon steel at relatively low concentrations.

The surface coverage, θ, can be calculated by θ=IE(%)/100. The isotherms of Langmuir, Frumkin, and Temkin were used for fitting data and the best results were found for Langmuir isotherm (Figure 3), which can be expressed in the following way [29]:

$$\frac{C}{\theta} = C + \frac{1}{K} \quad (2)$$

where C is the drug concentration, θ is the surface coverage and K is the equilibrium constant of adsorption. As can be seen in Figure 3, the plot of C/θ vs. C for the inhibitor is a linear plot with the correlation coefficient and slope close to 1, confirming the best fit of the polarization data to the Langmuir isotherm.

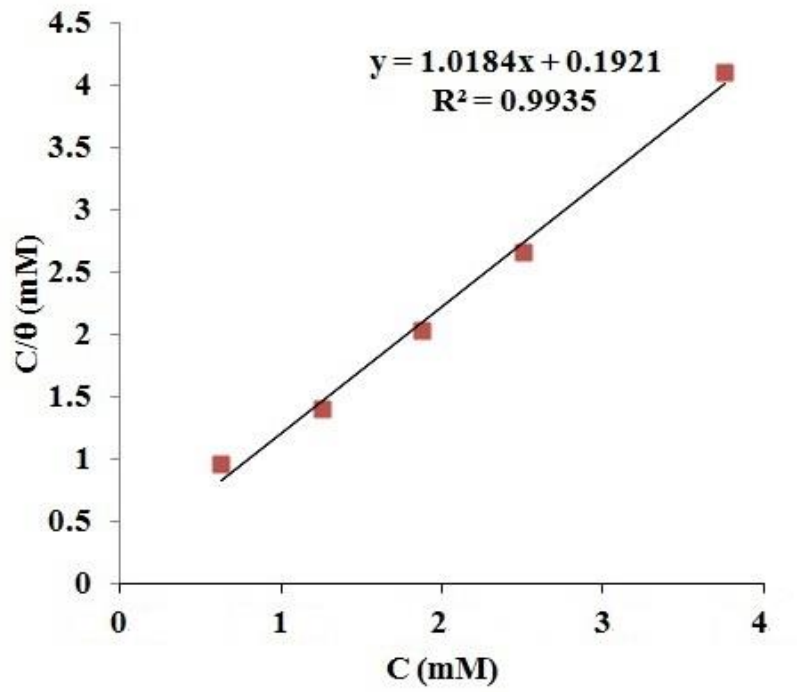

Figure 3. Langmuir adsorption isotherm of the inhibitor calculated by potentiodynamic polarization data for carbon steel in 3.5% NaCl solution saturated with CO_2.

3.2 Impedance measurements

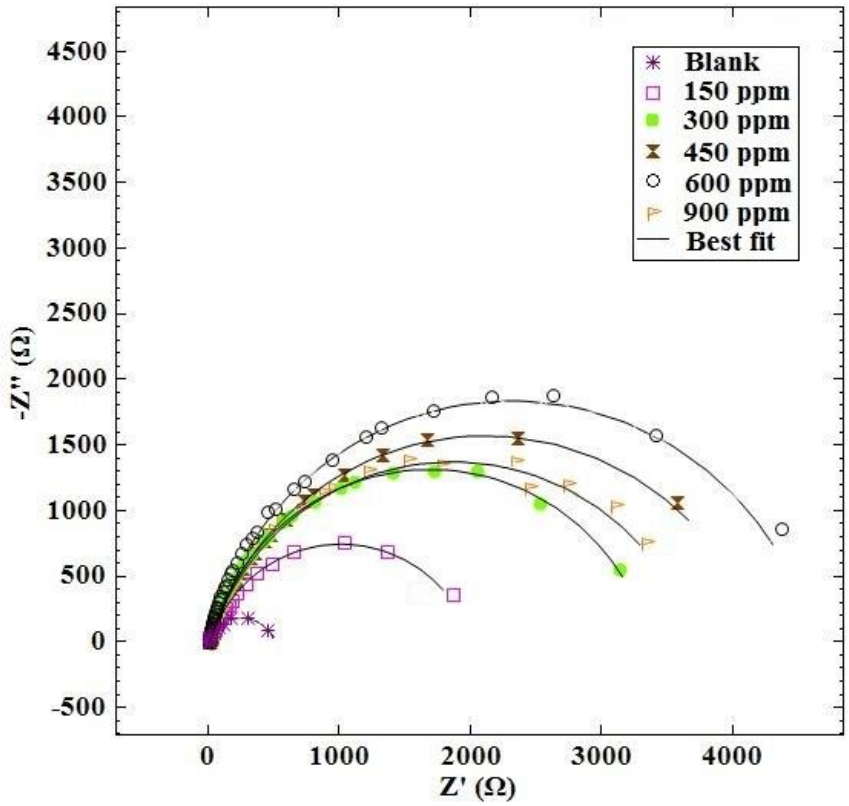

Figure 4. Nyquist plots for carbon steel in 3.5% NaCl solution saturated with CO_2 in the absence and presence of different concentrations of bupropion at 25°C.

The results of EIS measurements for carbon steel exposed to CO_2 saturated brine solutions containing different amounts of bupropion are shown in Figure 4. The investigated electrochemical system has resistive and capacitive elements since the Nyquist plots are in the form of semi-circles. According to the Nyquist plots, the charge transfer resistance (R_{ct}) increased with bupropion amount and reached its maximum value for 600 ppm of bupropion in the carbon dioxide saturated NaCl solution.

For investigating the details of electrochemical reactions occurring at the electrode/solution interface, an electrochemical equivalent circuit (Figure 5) was employed to fit the EIS results. A resistance of charge transfer (R_{ct}) and a constant phase element (Q_{dl}) were used in parallel to represent the corrosion process. The impedance value (Z_Q) of Q_{dl} element can be determined by the following equation [30]:

$$Z_Q = \frac{1}{Y_0(2\pi f\ j)^n} \quad (3)$$

where Y_0 is the Q constant, n is the exponent of Q element and f is frequency. Table 2 lists the parameters resulted from fitting of Nyquist spectra to the proposed equivalent circuit.

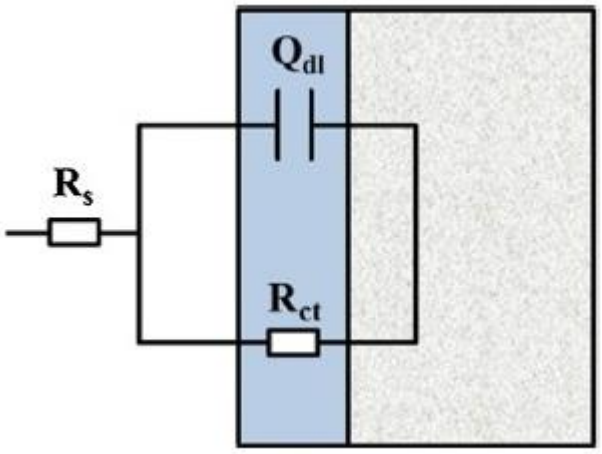

Figure 5. The equivalent circuit used to fit the experimental data.

Table 2. Impedance parameters and the corresponding inhibition efficiencies for carbon steel in 3.5% NaCl solution saturated with CO_2 in the absence and presence of different concentrations of bupropion drug at 25°C.

C /ppm	R_s/Ω.cm^2	R_{ct}/kΩ.cm^2	n	10^6 Y_0/Ω^{-1}.cm^{-2}	C_{dl}/μF.cm^{-2}	IE_{EIS}(%)
0	9.9	0.5	0.823	224	151	-
150	11.1	2.0	0.820	184	147	75.0
300	15.0	3.4	0.850	75.9	86	85.3
450	11.5	4.2	0.820	100	81	88.1
600	12.7	5.1	0.860	60.4	51	90.2
900	11.0	3.7	0.815	101	84	86.5

The electrical double layer capacitance (C_{dl}) was determined by the equation (4), providing the frequency of the maximum impedance imaginary component (f_{max}):

$$C_{dl} = Y_0 \left(2\pi f_{\max}\right)^{n-1} \quad (4)$$

It is evident from Table 2 that the increase of the drug concentration up to 600 ppm led to an increase in the R_{ct} values and a decrease in the C_{dl} values. This condition is due to the increased coverage of the steel surface by the drug, which can lead to decrease the aggressiveness of the CO_2 saturated brine solution. The IE% values in Table 2 were computed using the equation (5):

$$IE_{EIS}(\%) = \frac{R_{ct}^{'} - R_{ct}}{R_{ct}^{'}} \times 100 \quad (5)$$

where R_{ct} and $R_{ct}^{'}$ are the resistances of charge transfer for carbon steel in the CO_2 saturated brine solution before and after the addition of the drug, respectively. The increase of the drug concentration up to 600 ppm led to an increase in the IE values but there is a restriction in the sense that an additional increase in the drug amount up to 900 ppm made a decrease in the inhibition efficiency of the drug. The impedance IE% values (Table 2) are completely consistent with the polarization IE% values and confirm each other (Table 1).

The isotherms of Langmuir, Frumkin, and Temkin were employed for fitting the EIS data and the best results were found for Langmuir isotherm. As can be seen from Figure 6, the EIS results

confirmed that the adsorption of bupropion molecules can be fitted well to the Langmuir isotherm because both the regression parameter and the slope values are notably close to 1.

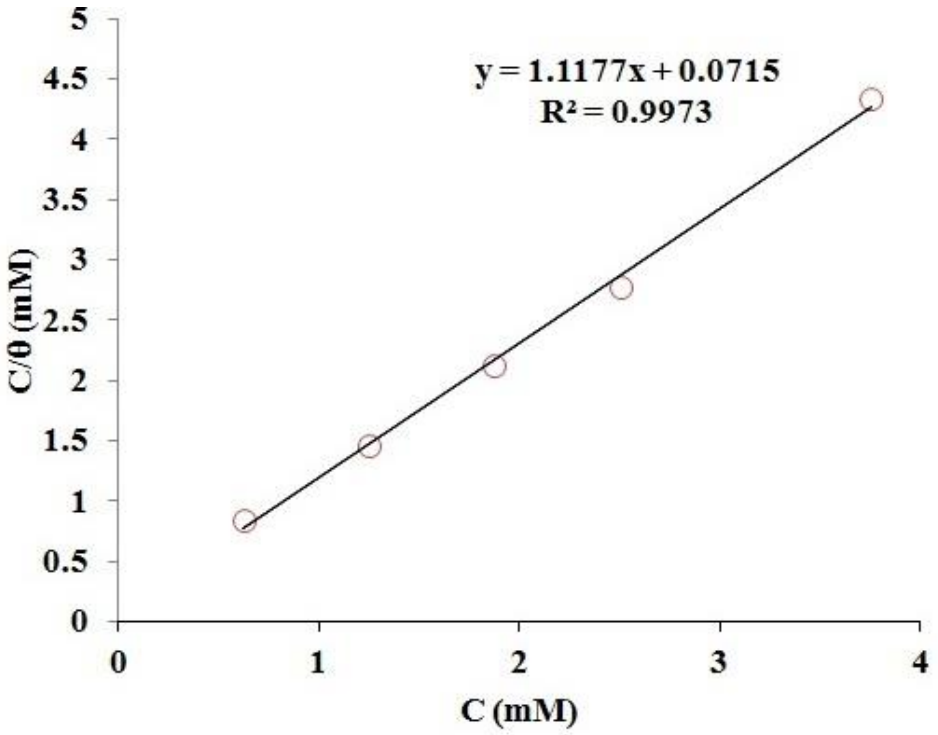

Figure 6. Langmuir adsorption isotherm of the inhibitor calculated by EIS data for carbon steel in 3.5% NaCl solution saturated with CO_2.

3.3 The effect of temperature

Polarization measurements in the range of 25 to 55°C were used to determine the activation energy (E_a) and some thermodynamic quantities for the carbon steel corrosion in the brine CO_2 saturated solution containing 100 ppm bupropion. The Tafel curves for carbon steel exposed to the carbon dioxide saturated brine solutions in the blank solution and 600 ppm drug concentration are demonstrated in Figure 7.

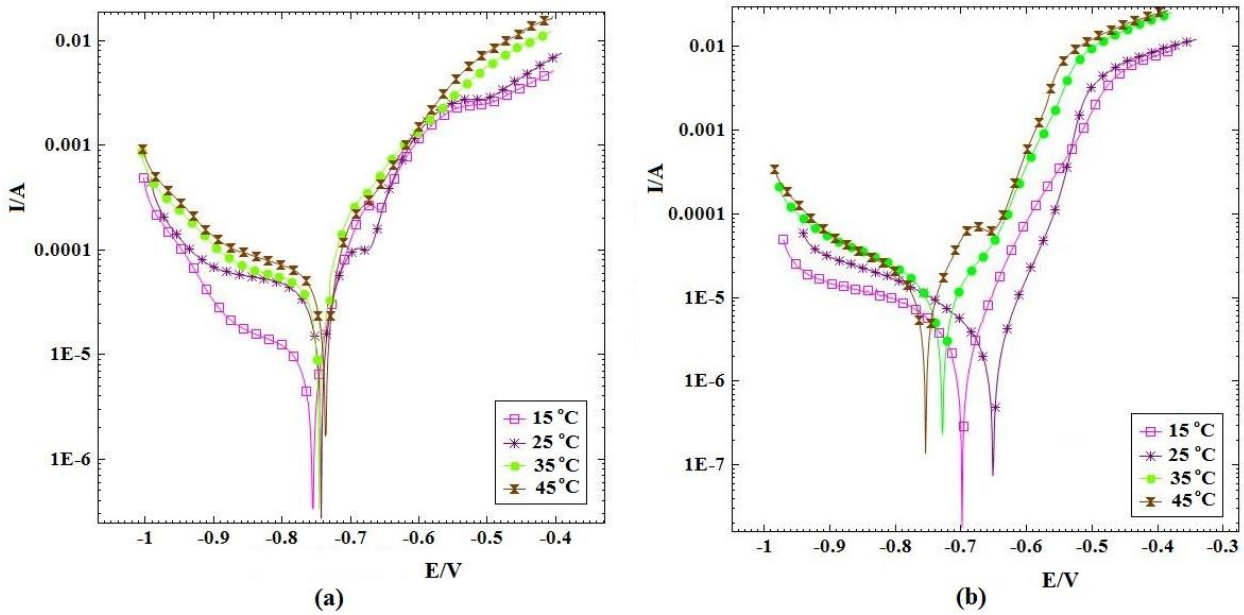

Figure 7. Effect of temperature on the polarization curves in 3.5% NaCl solutions saturated with CO_2 (a) without inhibitor and (b) in the presence of 100 ppm bupropion drug.

Table 3. Effect of temperature on the corrosion parameters of carbon steel in 3.5% NaCl solution saturated with CO_2 containing 600 ppm bupropion drug at 25°C.

C/ppm	T/°C	i_{corr}/μA.cm^{-2}	IE%	θ
0	15	13	-	-
	25	30.8	-	-
	35	51	-	-
	45	89	-	-
600	15	1.3	90.0	0.900
	25	2.8	90.9	0.909
	35	7.3	85.7	0.857
	45	14.1	84.2	0.842

Table 3 lists the corrosion factors obtained at various temperatures. The results showed an increase in the current density with increasing temperature. Generally, the current density increases with increasing temperature due to the shortening of the time lag between the adsorption and desorption of inhibitor molecules on the steel surface with increasing temperature [31]. Therefore, the steel surface is exposed to the corrosive solution for a longer period, and thereby the corrosion rate of steel is increased with increasing temperature.

It is evident from the polarization results that with an increase in temperature, a decrease in IE% has happened. A slight change in the IE values with the rise of temperature from 25 to 55°C proves the strong adsorption bonding of bupropion on the steel surface. It means that besides physisorption, the chemisorption of bupropion should also be involved.

Arrhenius equation can express the temperature influence on the corrosion rate according to equation (6):

$$i_{corr} = A\exp\left(\frac{-E_a}{RT}\right) \quad (6)$$

where i_{corr} is the corrosion current, A is the Arrhenius pre-exponential factor, E_a is the energy of activation, T is temperature (K), and R is the molar gas constant (8.314 J $K^{-1}mol^{-1}$). E_a values can be obtained from the slope ($-E_a/R$) of the Arrhenius plot [$\ln i_{corr}$ vs 1/T]. Figure 8 shows the Arrhenius plots for carbon steel electrode in 3.5% NaCl solutions saturated with CO_2 in the absence (blank) and the presence of bupropion. According to the slopes of the Arrhenius plots, it was revealed that the calculated E_a value in the presence of bupropion was larger than that in the absence of bupropion (61.8 kJ/mol vs 47.9 kJ/mol). The increase of E_a in the presence of bupropion indicates that the adsorption of bupropion on the steel surface leads to the formation of a physical barrier that reduces the steel reactivity in the electrochemical reactions of corrosion. Therefore, the rate of under deposit corrosion of carbon steel in the brine CO_2 saturated solutions decreased by bupropion drug.

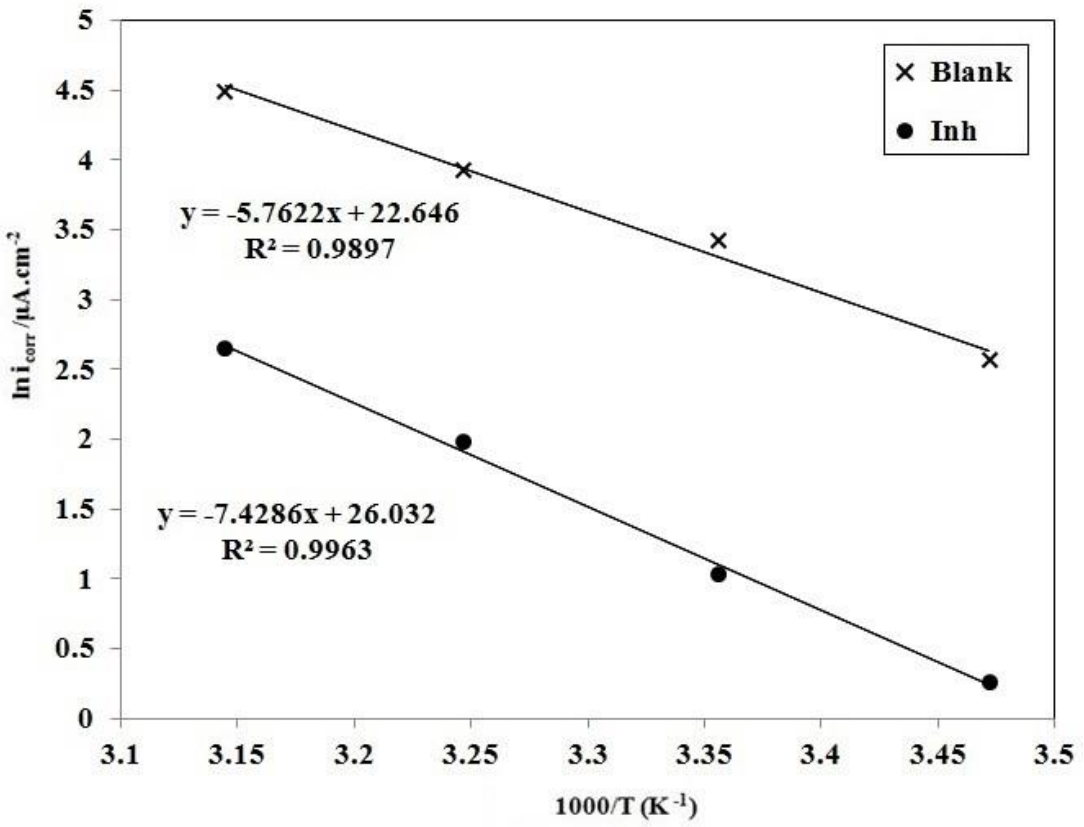

Figure 8. Arrhenius plots for carbon steel in 3.5% NaCl solution saturated with CO_2 in the absence and presence of 100 ppm bupropion.

The following equation can be employed for calculation of the Gibbs energy of inhibitor adsorption (ΔG_{ads}) on the carbon steel:

$$\Delta G_{ads} = -RT\ln(55.5K_{ads}) \quad (7)$$

where T is the temperature (K), R is the gas constant and K_{ads} is the adsorption equilibrium constant. The reciprocal of the intercept of the isotherm line is equal to the equilibrium constant of

adsorption (Figure 3). The values of K_{ads} and ΔG_{ads} are summarized in Table 4. Generally, if ΔG_{ads} values are more positive than −20 kJ/mol, it can be said that physical adsorption has occurred and if ΔG_{ads} values are more negative than −40 kJ mol^{-1}, it can be said that chemical adsorption has occurred. Therefore, it can be concluded from the obtained value for ΔG_{ads} that the adsorption of bupropion is not solely chemisorption or physisorption but involving comprehensive adsorption (both chemical and physical).

Table 4. The values of K_{ads} and ΔG_{ads} corresponding to polarization and EIS data in 3.5% NaCl solution saturated with CO_2

Drug	Polarization		EIS	
	K_{ads} (M^{-1})	ΔG_{ads} (kJ.mol^{-1})	K_{ads} (M^{-1})	ΔG_{ads} (kJ.mol^{-1})
Bup	5206	-31.2	13986	-33.6

The adsorption enthalpy, ΔH_{ads}, can be computed by the equation (8) [29]:

$$\ln\left(\frac{\theta}{1-\theta}\right) = \ln A + \ln C - \frac{\Delta H_{ads}}{RT} \quad (8)$$

where θ is the surface coverage calculated from θ=IE(%)/100, A is a constant, C is the inhibitor concentration, R is the gas constant, and T is temperature. A straight line is obtained from the plot of ln(θ/(1-θ)) versus 1/T at the constant amount of the drug as shown in Figure 9. The line slope is equal to $-\Delta H_{ads}/R$. The calculated value of ΔH_{ads} for inhibitor adsorption is gathered in Table 4. The exothermic adsorption behavior of the drug on the steel surface can be understood from the negative value of ΔH_{ads}.

The following equation was employed to calculate the adsorption entropy (ΔS_{ads}):

$$\Delta G_{ads} = \Delta H_{ads} - T\Delta S_{ads} \quad (9)$$

The obtained values for ΔS_{ads} are shown in Table 5. For accounting the negative value of ΔS_{ads}, it should be noticed that the adsorption of drug molecules from the solution is a quasi-substitution process between the drug molecules in the solution and the adsorbed water molecules on the steel surface [32]. The adsorption of the drug on the carbon steel surface is accompanied by the desorption of water molecules from the steel surface [33]. Before the adsorption of the drug on the carbon steel surface, the drug molecules can move randomly in the bulk solution, while after adsorption, the drug molecules can adsorb orderly on the alloy surface, and then, a decrease in the adsorption entropy can occur.

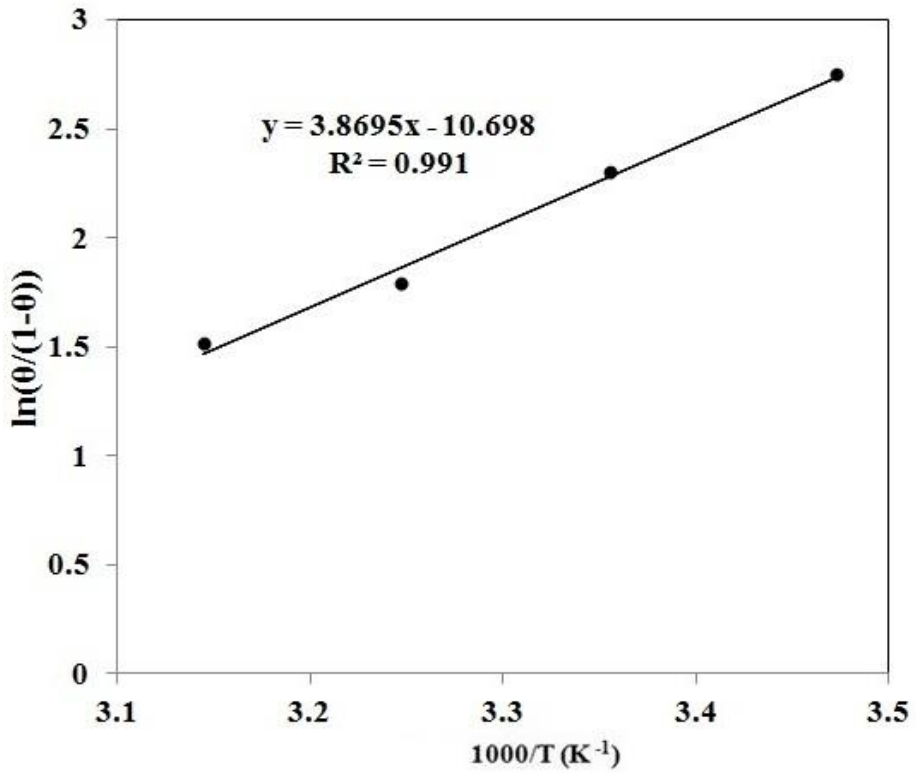

Figure 9. Plot of ln (θ/1–θ) vs. 1/T for carbon steel 3.5% NaCl solution saturated with CO_2 containing 100 ppm bupropion.

Table 5. Activation and thermodynamic parameters of adsorption obtained by potentiodynamic polarization measurements for carbon steel in 3.5% NaCl solution saturated with CO_2 in the absence and presence of 600 ppm bupropion drug at 25°C.

Drug	E_a ($kJ.mol^{-1}$)	K_{ads} (M^{-1})	ΔG_{ads} ($kJ.mol^{-1}$)	ΔH_{ads} ($kJ.mol^{-1}$)	ΔS_{ads} ($J.K^{-1}.mol^{-1}$)
Blank	47.9	-	-	-	-
Bup	61.8	5206	-31.2	-32.2	-3.4

3.4 Surface characterization

The optical microscope has been employed for evaluation of the effect of the drug on the surface morphology. The alloy specimens were immersed in the CO_2 saturated brine solutions both with and without 600 ppm drug concentration for 1 hour at room temperature. According to Figure 10, the steel specimen that was in contact with the drug showed a better condition in comparison to the one dipped in the blank solution. The specimen immersed in the drug solution showed less pitting corrosion in comparison with the blank sample. The steel surface was protected from corrosion due to the adsorption of the drug on the alloy surface.

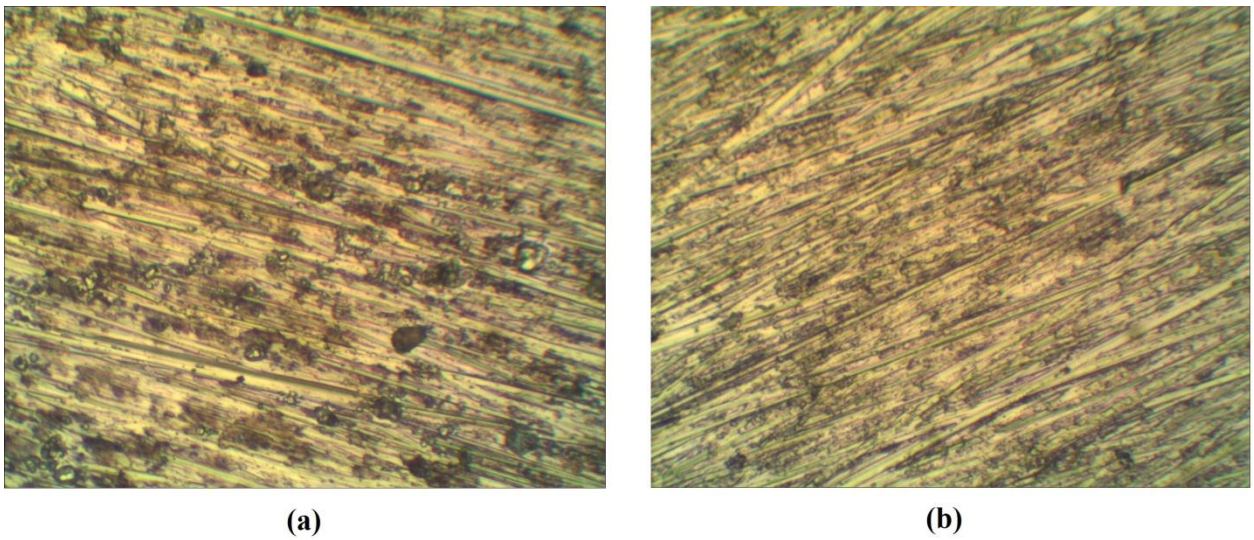

Figure 10. The optical microscopy images of sand-covered electrode after 1 h from immersion in CO_2 saturated brine solution in (a) the absence and (b) presence of 100 ppm bupropion drug.

4. CONCLUSION

Bupropion drug was employed as an inhibitor for under-deposit corrosion protection of carbon steel in CO_2 saturated NaCl solution. Potentiodynamic polarization curves showed that the drug reduced the corrosion of carbon steel. According to EIS measurements, the corrosion inhibition was caused by an increase in the charge transfer resistance at the steel-solution interface. The data acquired from the potentiodynamic polarization and the impedance measurements indicated that the adsorption of bupropion on carbon steel in brine solution saturated with CO_2 follows the Langmuir isotherm. The potentiodynamic polarization experiments at different temperatures suggested that bupropion can effectively minimize the corrosion effects of solutions on the alloy surface. The reason for the inhibition of alloy by bupropion was due to the adsorption of bupropion molecules on the alloy surface which was also evidenced by Langmuir isotherm study. The IE and ΔG_{ads} values obtained from the potentiodynamic polarization method showed acceptable compatibility with the data acquired from the EIS technique.

References

1. D. Han. R. J. Jiang, Y. F. Cheng. *Electrochim. Acta*, 114 (2013) 403.
2. Z. Mahidashti. M. Rezaei, M. P. Asfia. *Colloids and Surfaces A: Physicochemical and Engineering Aspects*, 602 (2020)
3. T. das Chagas Almeida. M. C. E. Bandeira. R. M. Moreira, O. R. Mattos. *Corros. Sci.*, 120 (2017) 239.
4. D. Dwivedi. K. Lepková, T. Becker. *RSC Advances*, 7 (2017) 4580.
5. R. F. Wright. E. R. Brand. M. Ziomek-Moroz. J. H. Tylczak, P. R. Ohodnicki. *Electrochim. Acta*, 290 (2018) 626.
6. D. A. Lopez. S. N. Simison, S. R. d. Sanchez. *Electrochim. Acta*, 48 (2003) 845.
7. X. Jiang, S. Nešić. *Corrosion/2009*, Paper No. 2414, NACE, Houston, TX (2009)

8. X. Jiang. S. Nesic. F. Huet. B. Kinsella. B. Brown, D. Young. *J. Electrochem. Soc.*, 159 (2012) C283.
9. S. N. Esmaeely. Y.-S. Choi. D. Young, S. Nešic. *CORROSION*, 69 (2013) 912.
10. W. Li. B. Brown. D. Young, S. Nešic. *CORROSION*, 70 (2014) 294.
11. R. D. Motte. R. e. Mingant. J. Kittel. F. Ropital. P. Combrade. S. Necib. V. Deydier, D. Crusset. *Electrochim. Acta*, 290 (2018) 605.
12. A. Kahyarian. B. Brown, S. Nesic. *Corros. Sci.*, 129 (2017) 146.
13. S. Hatami. A. Ghaderi-Ardakani. M. Niknejad-Khomami. F. Karimi-Malekabadi. M. R. Rasaei, A. H. Mohammadi. *The Journal of Supercritical Fluids*, 117 (2016) 108.
14. B. R. Linter, G. T. Burstein. *Corros. Sci.*, 41 (1999) 117.
15. M. Zeidabadinejad. M. Shahidi-Zandi. M. M. Foroughi, H. Asadollahzadeh. *Mater. Corros.*, 70 (2019) 1999.
16. J. Han. J. Zhang, J. W. Carey. *Int. J. Greenh. Gas Con.*, 5 (2011) 1680.
17. R. A. D. Motte. R. Barker. D. Burkle. S. M. Vargas, A. Neville. *Mater. Chem. Phys.*, 216 (2018) 102.
18. R. Feng. J. Beck. M. Ziomek-Moroz, S. N. Lvov. *Electrochim. Acta*, 212 (2016) 998.
19. M. Javidi. R. Chamanfar, S. Bekhrad. *Journal of Natural Gas Science and Engineering*, 61 (2019) 197.
20. H. H. Zhang, Y. Chen. *J. Mol. Struct.*, 1177 (2019) 90.
21. V. Pandarinathan. K. Lepková. S. I. Bailey, R. Gubner. *Corros. Sci.*, 72 (2013) 108.
22. R. Samiee. B. Ramezanzadeh. M. Mahdavian, E. Alibakhshi. *Journal of Cleaner Production*, 220 (2019) 340.
23. M. A. Amin, M. M. Ibrahim. *Corros. Sci.*, 53 (2011) 873.
24. E. McCafferty. *Corros. Sci.*, 47 (2005) 3202.
25. Y. Liang. C. Wang. J. Li. L. Wang, J. Fu. *Int. J. Electrochem. Sci.*, 10 (2015) 8072.
26. S. Hari Kumar, S. Karthikeyan. *Ind. Eng. Chem. Res.*, 52 (2013) 7457.
27. M. Lebrini. F. Robert. H. Vezin, C. Roos. *Corros. Sci.*, 52 (2010) 3367.
28. V. S. Sastri, Green Corrosion Inhibitors; Theory and Practice, John Wiley & Sons, (2011) New Jersey.
29. G. Golestani. M. Shahidi, D. Ghazanfari. *Appl. Surf. Sci.*, 308 (2014) 347.
30. M. G. Hosseini. M. Ehteshamzadeh, T. Shahrabi. *Electrochim. Acta*, 52 (2007) 3680.
31. E. A. Noor. *Corros. Sci.*, 47 (2005) 33.
32. I. Ahamad. R. Prasad, M. A. Quraishi. *Corros. Sci.*, 52 (2010) 933.
33. M. Şahin. S. Bilgiç, H. Yılmaz. *Appl. Surf. Sci.*, 195 (2002) 1